Experimental tests on achieving equilibrium in synthetic fluid inclusions: results for scheelite, molybdenite and gold solubility at 800°C and 200 MPa

Insa T. Derrey*[, 1], Moritz Albrecht[1], Evgeniya Dupliy[1], Roman E. Botcharnikov[1], Ingo Horn[1], Malte Junge[2], Stefan Weyer[1] & François Holtz[1]

[1] = Institut für Mineralogie, Leibniz Universität Hannover, Callinstr. 3, 30167 Hannover, Germany

[2] = Bundesanstalt für Geowissenschaften und Rohstoffe (BGR), Stilleweg 2, 30655 Hannover, Germany

* = corresponding author: i.derrey@mineralogie.uni-hannover.de

Abstract

Synthetic fluid inclusions formed in high P/high T experiments, which are subsequently analyzed with LA-ICP-MS, enable us to collect thermodynamic data to constrain metal transport in aqueous fluids as well as partitioning of metals between coexisting phases. The most essential prerequisite for such studies is to ensure that equilibrium conditions between liquid and solid phases are reached prior to the formation of synthetic fluid inclusions in the host mineral. Various methods have been proposed by different authors to achieve this goal, but to this point our knowledge on the best approach to synthesize equilibrated fluid inclusions under constrained pressure, temperature and compositional (P, T and X) conditions remains poor. In addition, information on the time needed to reach equilibrium metal concentrations in the fluid as well as on the timing of the onset of fluid inclusion formation in the host mineral are scarce.

The latter has been tested in a series of time-dependent experiments at 800°C and 200 MPa using scheelite ($CaWO_4$), molybdenite (MoS_2) and metallic gold as dissolving phases and using different approaches to optimize the formation of equilibrated fluid inclusions. Both fO_2 and fS_2 were fixed during all experiments using the Pyrite-Pyrrhotite-Magnetite buffer (PPM). As an intermediate in-situ quenching of the sample charge plays an important role in the synthesis of fluid inclusions, we further tested the efficiency of such an intermediate quench for re-opening fluid inclusions formed at 600°C and 200 MPa. Our results reveal that fluid inclusions start forming almost instantaneously and that equilibrium between fluid and solid phases occurs in the timescale of less than two hours for molybdenite and gold up to ca. 10 hours for scheelite. The best approach to synthesize equilibrated fluid inclusions at 800°C was obtained by using an intermediate quench on a previously unfractured quartz host. Experiments at 600°C showed similar results and illustrate that this should be the method of choice down to this temperature. Below 600°C pre-treatment of the quartz host (HF etching and/or thermal fracturing) becomes

important to produce large enough fluid inclusions for the analyses via LA-ICP-MS and special care must be taken to prevent premature entrapment of the fluid.

Fluids with 8 wt% NaCl in equilibrium with scheelite, molybdenite and gold at 800°C and 200 MPa have concentrations of ca. 7300 ppm W, 1300 ppm Mo and 300 ppm Au, respectively, which is in good agreement with results from other studies or extrapolation from lower temperatures. It can be concluded that the formation of synthetic fluid inclusions from an equilibrated fluid is possible, but different experimental designs are required, depending on the investigated temperature. In general, dissolution of solid phases seems to be much faster than previously assumed, so that experimental run durations can be designed considerably shorter, which is of great advantage when using fast-consuming mineral buffers.

Keywords: synthetic fluid inclusions, equilibrium, scheelite solubility in aqueous fluid, molybdenite solubility in aqueous fluid, gold solubility in aqueous fluid

Introduction

Magmatic and hydrothermal fluids play a crucial role in the formation of ore deposits, as they are the main transporting agents controlling mobilization and selective concentration of elements in the Earth's crust and, among others, metals of economic interest. Fluids trapped as fluid inclusions in magmatic and hydrothermal minerals provide direct insight into the genesis and evolution of natural fluids at the conditions of mineral growth or fracture healing. The correct reconstruction of natural conditions e.g., during ore formation, however, requires accurate and systematic quantification of the evolution of the fluid composition as a function of major parameters that control the properties of magmatic or hydrothermal systems. The main approach applied for such quantifications at high pressure (P) and temperature (T) is the experimental

synthesis of fluid inclusions which was described in the pioneering studies of Roedder and Kopp (1975), Shelton and Orville (1980) and Sterner and Bodnar (1984).

The development of laser ablation inductively coupled plasma mass spectrometry (LA-ICP-MS) techniques greatly improved the output of fluid inclusion studies, providing accurate quantitative analysis of major, but also trace and volatile element concentrations (Günther et al., 1998; Seo et al., 2011). In recent years, synthesis of fluid inclusions and subsequent LA-ICP-MS analysis have become the methods of choice in collecting thermodynamic data constraining metal transport in aqueous fluids and partitioning of metals between coexisting phases (e.g., Berry et al., 2006; Duc-Tin et al., 2007; Frank et al., 2011; Hack and Mavrogenes, 2006; Hanley et al., 2005; Heinrich et al., 1999; Lerchbaumer and Audetat, 2009; Loucks and Mavrogenes, 1999; Simon et al., 2006; Ulrich and Mavrogenes, 2008; Zajacz et al., 2010; Zhang et al., 2012).

One of the main challenges in such studies is to ensure that equilibrium conditions between liquid and solid phases were reached prior to the formation of fluid inclusions in the host mineral. For example, Hanley et al. (2005) stated that it was "impossible to demonstrate that brine-metal equilibrium was reached before fluid entrapment" in their experiments. There are two major kinetic factors influencing the entrapment of equilibrated fluid inclusions in experimental studies: a) the time necessary for the system to reach equilibrium with respect to all phases and buffer mineral assemblages (t_{equil}) and b) the time needed to heal cavities in the respective host minerals (quartz in most studies) (t_{heal}). Obviously, t_{heal} must be longer than t_{equil} to synthesize fluid inclusions representing equilibrium fluids.

Since healing of cracks and mineral growth can occur quite fast, various methods have been suggested to ensure achievement of equilibrium before fluid entrapment by delaying healing of the host mineral, by reopening previously healed cracks or by opening new cracks after a defined period of time. For instance, in their solubility study of NaCl and KCl in aqueous fluid, Sterner et

al. (1988) delayed crack healing of quartz by cycling pressure between 200 and 600 MPa in the first two hours of the experiment. With this technique, the compression and decompression of the fluid would lead to a continuous in- and out flux of the fluid through the cracks due to changes in fluid density, keeping the fluid in the cracks of the host mineral connected with the surrounding fluid. Using this approach, Sterner et al. (1988) were able to trap fluid inclusions with homogenous salt concentrations even at very high salinities. Subsequently it was proven that pressure cycling of about 100 MPa in total is sufficient to prevent fast healing of the cracks (P. Lecumberri-Sanchez, personal communication).

More recently, Li and Audetat (2009) developed a method to synthesize larger fluid inclusions under unfavorable growth conditions (e.g., low temperatures), which also provides a different method to constrain the time of system equilibration before onset of fluid entrapment using a *rapid heat/rapid quench cold seal pressure vessel* (RH/RQ-CSPV; design described in Matthews et al. (2003)). This method was used and tested by Zhang et al. (2012), when investigating the solubility of molybdenite in hydrothermal fluids. In a first step, they produced primary fluid inclusions by growing a new layer of quartz over an etched quartz piece. In a second step, some of the primary inclusions were reopened applying an intermediate quench using a rapid quench system (drop from 800°C to ± room temperature), which leads to in-situ fracturing of the quartz cylinder. Subsequently, the sample was replaced into the hot zone to trap secondary inclusions in the reopened cavities. Zhang et al. (2012) claimed that refilled inclusions trapped after the intermediate quench can be distinguished optically from primary inclusions by the intersection of cracks. Consequently, they could focus subsequent analysis of fluid inclusions via LA-ICP-MS on inclusions that formed after quenching and reheating. They noted that these fluid inclusions showed compositions considerably more constant than fluid inclusions from experiments without an intermediate quench.

A similar approach was used by Zajacz et al. (2010), who trapped two generations of synthetic fluid inclusions in a) a pre-fractured and b) a non pre-treated quartz chip in the same capsule, whereas the latter was only fractured in-situ by the intermediate quench (drop from 1000°C to ± room temperature after 24 h). They observed that the compositions of fluid inclusions in the pre-fractured and in the in-situ fractured quartz chips were usually identical within uncertainty, which supports their conclusion that equilibrium had been achieved before healing of the fractures in the pre-fractured chip.

To this point our knowledge on the best approach (among those described above) to synthesize equilibrated fluid inclusions remains poor. It is also not clear, which method is most suitable for certain P, T and X conditions. The pioneering studies applying an intermediate quench by (Zhang et al., 2012) and Zajacz et al. (2010) were performed at 600-800°C and 1000°C respectively and they differ in their outcomes concerning the ubiquitous need for an intermediate quench. Little is known about the efficiency of in-situ quenching at lower temperatures prevailing in the hydrothermal regime of ore deposits. In addition, kinetic studies to constrain the actual time necessary to equilibrate the fluid (t_{equil}) and trap it in the host mineral (t_{heal}) are still required.

In a series of experiments conducted at 800°C, 200 MPa and constant fO_2 and fS_2 (buffered by the assemblage Pyrite-Pyrrhotite-Magnetite: PPM) we tested the effects of quartz pre-treatment, pressure cycling and intermediate quenching on the formation and composition of metal-bearing fluid inclusions which were trapped from aqueous fluids coexisting with molybdenite (MoS_2), scheelite ($CaWO_4$) and gold at 800°C and 200MPa. To obtain a better understanding of the relationship between t_{heal} and t_{equil}, we conducted a series of time-dependent experiments (1 to 100 hours). We further applied an experimental protocol to test the efficiency of an intermediate quench and to distinguish fluid inclusions formed before and after an intermediate quench.

Finally, the results are used to discuss the solubility of molybdenite (MoS_2), scheelite ($CaWO_4$) and metallic gold in aqueous fluids.

Experimental Procedure

All experiments were conducted in RH/RQ-CSPVs of the design described in Matthews et al. (2003), using argon as pressure medium, at T = 400-800°C and P = 200 MPa. Uncertainties of temperature and pressure measurements are considered to be ≤ ±5°C and ±5 MPa, respectively. The external oxygen fugacity of our system was determined to be ca. NNO+2.3 (i.e., 2.3 log units above the Ni-NiO buffer; Berndt et al., 2001). For experiments using the PPM buffer, the phase assemblage after the run was analyzed by X-ray diffractometry to check if all the buffer minerals were still present at the end of the experiment, which they were in all cases. The capsule preparation for fluid inclusion synthesis generally followed the workflow described by Bodnar et al. (1985) with some modifications, which will be described below. Cylinders of 2.5 mm in diameter and ca. 2 mm in length were drilled out of inclusion-free alpine quartz. The cylinders were cleaned in concentrated HCl for 30 minutes and in an ultrasonic bath with distilled water for 5 minutes. After specific pre-treatments, described below and in Fig. 1, quartz cylinders were placed in Au capsules of ca. 25 mm length, 3.2 mm outer diameter and a wall thickness of 0.2 mm together with an 8 wt% NaCl-solution, different mineral powders, and silicagel to accelerate crack healing (for details see setup descriptions). The 8 wt% NaCl-solution was spiked with 398 ppm Rb and 400 ppm Cs (concentrations were calculated by gravimetry and confirmed by ICP-MS) and was used as internal standard during LA-ICP-MS analysis (see also method in Duc-Tin et al. (2007)).

Capsules were pressurized to 200 MPa at room T and rapidly moved to the preheated hot zone of the autoclave using the rapid heat device of the CSPV. The heating of the capsules to the target T occurred rapidly, within a few minutes, at isobaric conditions. In some experiments, the gold capsule was quenched quickly during the experiment by pulling the Au capsule from the hot end of the vertical autoclave to the water-cooled end to cause cracks within the quartz cylinder as a result of thermal stress (e.g., Li and Audetat, 2009). After this "intermediate quench" step of a few seconds, the capsule was moved back to the hot zone of the furnace. After a desired runtime, the autoclave was pulled out of the furnace and slowly cooled to room temperature (ca. 30°C/min in the temperature range 800 – 300°C) to avoid unnecessary cracking of the quartz chip. The capsules were weighed to check for potential leaks during the run. The recovered quartz cylinders were cleaned, dried and embedded in araldite to be cut and polished to chips of ca. 300 µm thickness.

Setup 1: Experimental approach for equilibration tests at 800°C

To identify the most reliable technique to synthesize fluid inclusions equilibrated with metal-bearing phases, we compared the methods of Sterner et al. (1988), Zhang et al. (2012) and Zajacz et al. (2010) that were described above. Each test was conducted in a Au capsule containing molybdenite (MoS_2) and scheelite ($CaWO_4$) as a metal sources.

- *Experiment A:* For pressure cycling experiments, we used quartz cylinders that were previously heated to 350°C in a muffle type furnace, quenched in distilled water, dried and immersed in concentrated (40 wt%) hydrofluoric acid (HF) for 10 minutes to widen the cracks. According to the design in Fig. 1a, one quartz cylinder was placed in a Au capsule together with 25 µl of NaCl solution, 5-15 mg of each mineral powder, ca. 50 mg PPM

buffer (mixed in weight ratio 1 Pyrite : 3 Pyrrhotite : 1 Magnetite) and 3-5 mg of silicagel powder.

- *Experiment B:* Capsules for experiments with the design of (Zhang et al., 2012) were prepared in the same way, but quartz cylinders were not cracked thermally and only immersed in concentrated HF for 30 minutes to produce cavities along the rim of the quartz cylinder (Fig. 1b).
- *Experiment C:* Capsules that were designed according to Zajacz et al. (2010) contained two quartz cylinders on top of each other (Fig. 1c), one was pre-treated in the same way as in *Experiment A* (*C_1*) and one was not pre-treated, except for HCl cleaning in an ultrasonic bath (*C_2*).

Experiment A was started as described above. Once the sample was moved into the hot zone, which was pre-heated to 800°C, pressure (which was previously set to 200 MPa) was cycled from 150 MPa to 250 MPa for five times every 10 minutes for a total time span of 8 hours. After pressure cycling, pressure was held constant at 200 MPa for three days before the capsule was quenched slowly.

For *experiments B and C*, the capsules were moved into the hot zone of the pre-heated (800°C) and pre-pressurized (200 MPa) autoclave. After two days at constant P and T, an intermediate quench was conducted for approximately 10 seconds. The capsules were then left in the hot zone for another three days before quenching slowly.

Setup 2: Experimental approach to test the efficiency of an intermediate quench for re-opening of fluid inclusions formed at 600°C

In this approach, we tested to which extent the application of an intermediate quench is successful for re-opening fluid inclusions. In the first phase of the experiment, the temperature

212 was fixed to 600°C (200 MPa). After the intermediate quench, temperature was set to 400°C
213 before the capsule was reentered into the hot zone. In this way, we were able to distinguish easily
214 between fluid inclusions formed before (600°C) and after the intermediate quench (400°C) via
215 microthermometry. To investigate the possible influence of different quartz pre-treatment each
216 experiment was performed with two capsules: one containing a quartz cylinder pre-treated as in
217 *experiment A* (cracked at 350°C plus 10 min in HF) and one containing quartz pre-treated in the
218 traditional way described by Sterner and Bodnar (1984), who only cracked the quartz thermally at
219 350°C. With the two different types of pre-treated quartz cylinders, a series of 2 x 3 Au-capsules
220 were prepared containing 2.5, 5 and 10 wt% NaCl solution and 2-6 mg silicagel powder. After 7
221 days at 600°C, the samples were quenched rapidly and left in the cold zone of the autoclave until
222 the furnace had cooled nearly isobarically to 400°C. The samples were then placed back into the
223 hot end of the autoclave, where they were left for 13 days at 400°C before the experiment was
224 terminated with a slow quench.
225
226 **Setup 3: Dissolution kinetics and time dependent experiments**
227 To assess the time necessary to form inclusions in pre-cracked quartz and to equilibrate
228 molybdenite, scheelite and gold with fluids at 800°C, we designed a series of experiments at 200
229 MPa with runtimes ranging from 1.8 to 100 hours. For each investigated run duration two gold
230 capsules were prepared, one containing molybdenite and the other one containing scheelite as
231 mineral powder. The capsule design was such that one quartz cylinder (pre-treated as in
232 *experiment A*: thermally cracked at 350°C plus 10 min in concentrated HF) was placed in a Au
233 capsule together with 25 µl of NaCl solution, 5-15 mg of the respective mineral powder, ca. 50
234 mg PPM buffer and 3-5 mg of silicagel powder. Experiments were run as described above
235 without an intermediate quench and the results compared to experiments from Setup 1.

236 Accounting for the exponential character of dissolution processes, the different runtimes were
237 chosen to be evenly distributed when plotted logarithmically.
238
239 **Analytical Procedure**
240 Fluid inclusions recovered from equilibration test and time dependent runs were analyzed for
241 their major and trace element contents by LA-ICP-MS. We applied a technique which is based on
242 the combination of a UV-femtosecond-laser (*Spectra Physics*) with a heating-freezing cell and a
243 high-resolution magnetic sector-field ICP-MS (*Element XR, Thermo Scientific*) (for details see
244 Albrecht et al., 2014). The in-house build laser ablation system is operating in the deep UV range
245 at 194 nm. A slightly modified INSTEC^{TM} heating-freezing stage with an adjusted cell volume of
246 3 cm³ is used as laser cell. Helium mixed with 2 vol% hydrogen (to adjust the hydrogen flow rate
247 to ca. 5-6 ml/min as suggested by Guillong and Heinrich (2007)) was used as sample-chamber
248 gas and mixed with argon downstream. Analyses were performed at temperatures of -60°C,
249 guaranteeing completely frozen fluid inclusions prior to the ablation, which resulted in an
250 excellent control on the opening of the inclusions and considerably longer signal analysis time.
251 The analytical uncertainty of the method is considered to be 10-30% for most elements as
252 described by Albrecht et al. (2014). NIST SRM 610 glass was used as external standard (using
253 reference values of the GeoReM database (Jochum et al., 2005)) and measured with a repetition
254 rate of 10 Hz after every fourth inclusion. Laser repetition rates for fluid inclusion analyses have
255 been 5 – 10 Hz, depending on the depth of the inclusion, with higher rates for deeper (up to 50
256 µm) inclusions. To evaluate the acquired data, the SILLS data reduction software (Guillong et al.,
257 2008) was used, which is particularly suitable for the interpretation of fluid inclusion signals. The
258 known Cs concentration of the starting fluid was used for internal standardization and compared
259 to Rb and Na concentrations, which were also known. Fluid inclusion analyses in which the

Rb/Cs-ratio deviated by more than 10% and/or the Na/Cs-ratio by more than 20% were discarded as they are considered to represent analyses of poor quality (Zhang et al., 2012). Figure 2 shows a representative spectrum of a fluid inclusion analysis.

Fluid inclusions from experiments testing the efficiency of an intermediate quench were examined by microthermometry using a *Linkam FTIR600* heating-freezing stage. About 30 fluid inclusions were analyzed from each quartz chip. Final ice melting temperatures (T_m) were determined to check, if the resulting salinities corresponded to the weight salinities of the different starting fluids. Homogenization temperatures (T_{hom}) were determined to distinguish between fluid inclusions that formed prior to (600°C, 200 MPa) and after (400°C, 200 MPa) the intermediate quench. The expected T_{hom} were calculated using the SoWat code, which comprises the data of Driesner (2007) and Driesner and Heinrich (2007).

Results

Setup 1: Equilibration tests

All experimental run products from setup 1 contain abundant synthetic fluid inclusions varying in size from a few µm to more than 100 µm (e.g. Fig. 3). Whereas the experimental designs *B* and *C_1* produced a large amount of fluid inclusions with many of them in the preferable range for LA-ICP-MS (>10 µm), designs *A* and *C_2* show on average smaller and less fluid inclusions, but still abundant and large enough for analysis. Quartz chips made from cylinders from design *A* (pressure cycling) deviate from the usually rectangular shape after the experiments (Fig. 4).

The outcome of the different experimental designs to achieve equilibrium between solid phases and fluid are shown in Figure 5 and average values including standard deviations summarized in Table 1. Metal concentrations in fluids from all experimental designs are in the same range

284 within error and correspond to approximately 6000 ppm W for scheelite-bearing samples, 1300
285 ppm Mo for molybdenite-bearing samples and 300 ppm Au, clustering within a standard
286 deviation range of ca. 10 – 25% (cf. Tab. 1). The pressure cycling experiment (design *A*),
287 however, resulted in fluid inclusions with a larger range in the analyzed concentrations (at least
288 for W and Au).
289
290 **Setup 2: Role of the intermediate quench**
291 Fluid inclusions in quartz cylinders, which were not only cracked at 350°C but additionally
292 etched in concentrated HF are considerably larger (many inclusions > 20 µm; Fig. 3b) than those
293 from cracked cylinders without etching (usually < 20 µm, mostly < 10 µm; Fig. 3a). Furthermore,
294 no fluid inclusions that formed at 400°C were measurable in the latter cylinders. Inclusions that
295 formed in cracked and etched quartz cylinders show clearly two distinct groups with different
296 T_{hom}, which can be related (after pressure correction according to Driesner and Heinrich (2007))
297 to the two different formation temperatures of 600°C and 400°C (Fig. 6, Table 2). Both
298 generations could be distinguished easily by their different T_{hom} via microthermometry, but it was
299 not possible to distinguish the two generations optically, which is in contrast to the observation
300 Zhang et al. (2012), who used an identical temperature of 800°C prior and after the intermediate
301 quench. Fluid inclusions that formed at 600°C and 400°C could not be distinguished according to
302 their distribution in the quartz chip, as they occur adjacent to each other in all parts of the quartz
303 (from center to rim) with no obvious relation to certain areas or surfaces.
304
305 **Setup 3: Time dependent experiments**
306 Figure 7 depicts the results of the time dependent experiments (summarized in Table 3). Even in
307 the two shortest runs (1.8 h and 3.2 h) abundant fluid inclusions were trapped in the quartz

crystals, but they are considerably smaller (mostly < 10 μm, few inclusion between 10 – 20 μm) than those from longer runs, resulting in larger analytical errors due to insufficient counting statistics. In this experimental series, no intermediate quench was performed, so that the large range in concentrations of one element in fluid inclusions within one sample is primarily interpreted to represent true variations due to different times of entrapment rather than analytical error. Fluid inclusions which formed early in the experiment are expected to show non-equilibrated metal concentrations.

Figure 7 demonstrates that the highest Mo and Au concentrations are in the same range in all experiments (except for the shortest run where Mo concentrations are higher), independent on the run duration. This indicates that equilibration of fluids with molybdenite and gold is fast and reached within the first few hours of the experiment. On the other hand, the maximum W concentrations increase within the first hours and remain constant after approximately 10 hours.

Discussion

In the following the outcome of the experiments are used to discuss the best approach for the synthesis of equilibrated fluid inclusions.

Size and number of fluid inclusions

When preparing mineral cylinders to trap hydrothermal fluids during an experiment, we suggest a pre-treatment of cylinders by both thermal cracking (10 min. at 350°C followed by quench in room temperature distilled water) and immersion in concentrated HF for 10 minutes. If quartz is pre-treated in this way, the formation of the highest number of fluid inclusions (compared to pre-treatment with HF only) is observed and fluid inclusions have a considerably larger size (compared to quartz that was only thermally cracked). This becomes especially important in

experiments at lower temperatures because fluid inclusions are usually too small for LA-ICP-MS (ca. < 10 µm) or even microthermometry (ca. < 5 µm) under these conditions. Furthermore, our experiments from setup 1 showed that fluid inclusions in both thermally cracked and HF-etched quartz are more prone to in-situ fracturing by an intermediate quench, which becomes especially important in experiments with long equilibration times.

Dissolution kinetics

From our time dependent experimental series (setup 3) for the dissolution of molybdenite, scheelite and gold we gained two main insights, which are: 1) that fluid inclusions start to form almost instantaneously (< 1.8 h) under the applied conditions and 2) that the dissolution of the investigated metal-bearing phases at 800°C is fast. As the metal concentrations from setup 3 are very similar to those from setup 1 (equilibration tests; cf. Fig. 5 and 7), it can be concluded that equilibrium of the fluid was reached in the time scale of a few hours (< 1.8 h to ca. 10 h). Thus, although the fast formation of inclusions at 800°C has a negative influence on the formation of equilibrated fluid inclusions, this effect is reduced by the fact that metal dissolution is comparably fast. The fast entrapment of fluid inclusions in quartz emphasizes the importance of a rapid heating autoclave, which keeps the time until the experimental temperature in the capsule is reached at a minimum.

It is known that quartz solubility depends on the salinity of the fluid (e.g., Akinfiev and Diamond, 2009; Newton and Manning, 2000), which might possibly influence the velocity of crack healing. Our time dependent series was conducted with an 8 wt% NaCl fluid. According to Newton and Manning (2000) at this salinity and our experimental P/T conditions (800°C, 200 MPa) quartz solubility is close to its maximum. Thus, any deviation in the salinity of the fluid would lead to a

355 decrease in quartz solubility. So if there was an effect it would likely be a delay of crack healing,
356 which would be advantageous for reaching equilibrium prior to entrapment of the fluid.
357 Whereas molybdenite and gold appear to dissolve and equilibrate very fast (faster than our
358 shortest experiment, with an apparent oversaturation of molybdenite in the shortest run),
359 maximum W concentrations from scheelite dissolution rise from ca. 2400 ppm after 1.8 h to ca.
360 7300 ppm within the first 10 hours, before they remain constant (Fig. 7). This might be due to the
361 more covalent bonding of W in the tungstate molecule and concomitant slower dissolution
362 kinetics compared to Mo from molybdenite and Au from native gold. Additionally, the different
363 crystal structure and chemical composition of scheelite, including Ca as an additional cation,
364 likely influences dissolution kinetics. Fast equilibration of Au concentration was also shown by
365 Benning and Seward (1996), who determined Au equilibration times of roughly 3 days at 150°C,
366 1.5 days at 200°C, 1 day at 300°C and "a few hours" at 500°C. Exponential extrapolation of this
367 dataset results in an equilibration time of <1 h at 800°C, which is in perfect agreement with our
368 findings.
369 Our results indicate that time dependent series similar to ours are useful to get an estimate of
370 optimal run durations needed to equilibrate the system of interest with respect to all phases
371 including buffers. Findings of Zajacz et al. (2010) showed that there are cases where equilibration
372 might take longer, e.g. due to a slowly adjusting buffer. In their experiments, this occurred in a
373 case study where a large amount of H_2 had to diffuse out of the gold capsule to achieve redox
374 equilibrium and crack healing was apparently faster than the time needed to equilibrate the
375 system. As a result, the compositions of fluid inclusions were different in a pre-treated and in a
376 previously unfractured and in-situ quenched quartz chip. However, in most systems metal
377 concentrations seem to equilibrate fast enough to be studied by synthetic fluid inclusion
378 technique, which is also supported by the findings of Simon et al. (2007). According to them,

379 quartz crack healing is slow enough to allow the entrapment of fully equilibrated fluids at 800°C
380 and 100 MPa in the haplogranite – magnetite – gold – NaCl – KCl – HCl – H_2O system, but no
381 estimate of crack healing times is given. Simon et al. (2007) further highlighted the importance of
382 a low thermal gradient (≤±5°C) across the experimental charge to prevent the formation of a
383 rapidly precipitating primary quartz overgrowth. We determined a temperature gradient of ≤±2°C
384 over the length of 3 cm for our experimental charges.
385
386 **Importance of intermediate quench**
387 As shown by Zhang et al. (2012), Zajacz et al. (2010) and this study, an intermediate quench (i.e.,
388 in-situ quartz cracking) after a long enough equilibration time will lead to the smallest scatter in
389 metal concentrations from the resultant fluid inclusions. In our equilibration tests at 800°C, the
390 best results were achieved with fluid inclusions formed after an intermediate quench in quartz
391 cylinders which were not pre-treated (Fig. 5, design *C_2*). This could be expected, as this
392 approach is the only design in which inclusions cannot form before the intermediate quench (we
393 did not observe formation of quartz overgrowth which could have led to entrapment of primary
394 fluid inclusions). The drawback of this method is that it gets increasingly less effective at lower
395 temperatures. Thus, the design *C_2* is appropriate and recommended for experiments at rather
396 high temperatures (1000°C, Zajacz et al. (2010); 800°C, this study).
397 From our experience, it was only possible to induce enough cracks in quartz and to produce fluid
398 inclusions sufficiently large for LA-ICP-MS by an intermediate quench down to a temperature of
399 ca. 600°C. Below 600°C only few and very small inclusions form in the unfractured quartz and
400 such inclusions were not suitable for LA-ICP-MS. Figure 3 c) and d) show the different
401 appearance of fluid inclusions formed in an unfractured quartz chip by an intermediate quench at
402 800°C and 600°C, respectively. Both, the abundance and size of synthetic fluid inclusions

403 decrease rapidly with decreasing temperature. Thermal cracking is further hindered by the use of
404 double capsules (Eugster, 1957 and following), which makes in-situ cracking less effective than
405 in single capsules. Therefore, in-situ cracking of initially unfractured quartz by an intermediate
406 quench should be the method of choice for synthesis of fluid inclusions at high temperatures, but
407 it is less useful at temperatures below 600°C. In any case, it is recommendable to add a pre-
408 treated quartz (of design *B* or *C_1*) to the capsule to ensure the formation of sufficient fluid
409 inclusions of optimal size, which can then be compared to inclusions from initially unfractured
410 quartz. In our experiments, the results from design *B* and *C_1* show only minor deviation from
411 results of design *C_2* with not pre-treated, in-situ cracked quartz, but a larger range in the
412 individual analyses (Fig. 5). However, both designs are recommended for experiments below
413 600°C, as they will ensure the formation of adequate fluid inclusions down to at least 400°C. Our
414 experiments testing the re-opening of fluid inclusions after an intermediate quench showed that
415 in-situ quenching and subsequent formation of new fluid inclusions works down to at least 600°C
416 (Fig. 6B). The replacement of fluid inclusions, however, only occurs partly and we were not able
417 to distinguish optically between fluid inclusions that formed prior to and after the intermediate
418 quench. Thus, the interpretation of LA-ICP-MS of fluid inclusions that formed after the
419 intermediate quench may be difficult. The yield of equilibrated fluid inclusions might be
420 increased by quenching the sample in-situ several times in short succession (R. Linnen, personal
421 communication).
422
423 **Limitations of pressure cycling**
424 Equilibration design *A* (pressure cycling) does not seem suitable for our conditions, as the metal
425 concentrations in fluid inclusions show the largest range in concentrations (but comparable
426 values in average, Fig. 5). This is interpreted to be due to several factors. One possible reason

427 could be that the duration of pressure cycling (8 hours) was too short for the metal concentrations
428 to equilibrate. But this interpretation is not confirmed by the results from the time dependent
429 experiments, at least for Mo and Au (Fig. 7). A second possible explanation is that some
430 inclusions with low metal concentrations formed in the very early stages of the experiment and
431 were not re-opened despite of pressure cycling. Possibly, a higher total pressure difference is
432 needed after all (as applied by Sterner et al. (1988)) to change the fluid density enough to prevent
433 the cracks from healing. Yet another explanation would be that some inclusions decrepitated as a
434 result of pressure variation, which may explain anomalous high and low metal concentrations.
435 The observed change in shape of the quartz cylinders after the experiment (Fig. 4) might be due
436 to deformation of the quartz during the experiment, which may indicate that partial decrepitation
437 occurred during pressure cycling. This would imply that a temperature of 800°C is too high for
438 pressure cycling experiments, as the quartz crystal becomes ductile and deforms in response to
439 the oscillating pressure. However, no decriptitation of fluid inclusions was observed under the
440 microscope and the observed change in shape could also be the result of quartz overgrowth along
441 preferred crystallographic orientations. Fluctuations in quartz solubility during pressure cycling
442 may have resulted in enhanced dissolution and reprecipitation of quartz. At lower temperatures
443 this effect should also be minimized so that, with an appropriate cycling period and pressure
444 difference, this method might be the method of choice for some applications at low temperatures,
445 as e.g., described by Sterner et al. (1988). The use of a different host mineral, which is less
446 soluble than quartz at high temperatures, could possibly expand the applicability of this method
447 to higher temperatures.
448
449 **Au, Mo and W concentrations in fluids in equilibrium with Au metal, molybdenite and**
450 **scheelite**

As Au and Mo concentrations in fluid inclusions from all experimental designs are identical within error (except for the shortest run from setup 3, where Mo concentrations are higher) and are in the same range as the maximum concentrations determined in the time dependent experiments, they are interpreted to represent concentrations in 8 wt% NaCl fluids in equilibrium with Au metal and molybdenite at 800°C, 200 MPa and PPM buffered conditions. Comparing maximum W concentrations from the equilibration tests and time dependent experiments, it is noticeable that W concentrations are slightly lower in the former (ca. 6100 ppm versus ca. 7300 ppm). This might be a result of the relatively large scatter of W concentrations (standard deviation ca. 2000 ppm) in the time dependent experiments, which were performed without an intermediate quench. However, the difference in the capsule design between the two setups is that in the equilibration tests scheelite and molybdenite were placed together in the same capsule, whereas capsules with either scheelite or molybdenite were prepared for the time dependent experiments. Therefore, W solubility could be dependent on Mo in the system, whereas Mo concentrations do not change notably between both experimental designs and are in the order of 1300 ppm, which is also in good agreement with the data from Zhang et al. (2012, see *2 in Fig. 5), who performed experiments with molybdenite only and who reported average Mo concentrations for experiments of the same design of 1200 to 1510 ppm. This may indicate that W and Mo, both of which are hard Lewis acids, compete for the same ligands (e.g., OH^-, O^{2-}, Cl^-) but that Mo forms the more stable complexes and is thus complexed preferentially, possibly due to the slightly higher difference in electronegativity with respect to oxygen.

Figure 5 (*1) also shows W concentration extrapolated from scheelite solubility data from Foster (1977) obtained between 252 and 529°C in the pressure range 100-200MPa. Assuming a linear correlation of logW(ppm) vs. 1000/(T in K), a least square extrapolation resulted in a value of ca. 1200 ppm (or 1900 ppm if two obvious outliers are discarded). This is lower by a factor of ~ 3-5

475 when compared to our data (fluids in equilibrium with scheelite only) and the possible variation
476 may be due to the use of a different buffer (Msk-Kfs-Qz) and salt in the solution (1 M KCl,
477 which corresponds to 7.17 wt% KCl), but likely also due to quenching problems and the
478 formation of precipitates, as Foster (1977) sampled the fluid directly from the capsule. Loucks
479 and Mavrogenes (1999), who applied the synthetic fluid inclusion approach investigated the
480 solubility of gold. Extrapolation of their Au concentrations from experiments in the range of 625
481 to 725°C led to a value of roughly 220 ppm Au (Fig. 5, *3), which is slightly lower than our
482 results of ca. 300 ppm. Even though their experiments were performed under the same buffer
483 conditions (PPM), other experimental conditions differed, which may explain the small
484 discrepancy. In particular, the experiments were conducted at 110 MPa and they used a 1 m HCl
485 solution. Extrapolation of Au concentrations determined via direct fluid sampling from the
486 capsule by Gibert et al. (1998) in the range of 350 to 450°C leads to a value of roughly 40 ppm
487 Au, which is considerably lower than our results. The experiments of Gibert et al. (1998) were
488 performed under the same buffer conditions (PPM), but were conducted at 50 MPa and the
489 authors additionally used the Msk-Kfs-Qz buffer and a 0.5 M KCl solution. The lower
490 concentration might also stem from quenching problems and the formation of quench
491 precipitates. In general, extrapolation to higher temperatures and pressures must be applied with
492 caution, as metal complexation at low P-T conditions may be different from that at higher P-T
493 (Pokrovski et al., 2015).
494 It was previously mentioned that analyses from the shortest time dependent experiment are
495 subject to a large analytical error due to the small size of produced fluid inclusions. Therefore,
496 the slightly higher Mo concentrations in the experiment compared to the longer durations might
497 be solely explained by bad counting statistics. It cannot be ruled out though that Mo experiences
498 a true early oversaturation, which might be due to a lower fS_2 in the fluid before the Pyrite-

Pyrrhotite-Magnetite buffer has equilibrated. Following Chatelier's principle a lower fS_2 would lead to a distortion of the dissolution equilibrium as proposed by Zhang et al. (2012) in favor of the side with the dissolved species:

$MoS_2(s) + lH_2O + mO_2 = H_{2l}MoO_{l+2m}S_{2-2n}(aq) + nS_2$

Implications

In this study we confirmed that synthetic fluid inclusions are a successful tool to probe fluids in experiments at high temperatures and pressures without the problem of fluid quenching. Solubilities of solid phases in different fluids can be determined under various conditions, including the possibility to access partitioning data of elements between various phases. However, the implication of the discussion is that there is currently no universal and perfect experimental design for the synthesis of equilibrated fluid inclusions. Depending on the investigated temperature, pressure, equilibrating phases and host mineral in the experiments, different designs need to be applied to obtain reliable result.

For experiments with T≥600°C, we recommend the use of our experimental design *C*, as from our experience this design produces results of the best quality. In particular, applying an intermediate quench (or possibly several) after a well-defined equilibration time is strongly recommended. Time dependent experiments showed that mineral dissolution is considerably faster than usually assumed (e.g. Hanley et al., 2005; Simon et al., 2007; Zhang et al., 2012). The dissolution of scheelite takes slightly longer than that of molybdenite and gold, but is still in the order of hours rather than days at 800°C. As a consequence, experimental durations can be designed much shorter than previously done, which is a great advantage when using fast consuming solid mineral buffers. Nevertheless, equilibration times of the used buffer also need to

522 be taken into account when deciding on the length of the experiment prior to the intermediate
523 quench.
524 For experiments distinctly below 600°C, the use of an unfractured additional mineral cylinder can
525 be discarded, as it does not yield fluid inclusions that are large enough for LA-ICP-MS analysis.
526 It is, however, possible to produce adequate fluid inclusions down to at least a temperature of
527 400°C in doubly pre-treated quartz cylinders. But care must be taken in estimating t_{heal} and t_{equil},
528 which will be longer than at higher temperatures. Below 400°C we were not able to produce fluid
529 inclusions which were suitable for LA-ICP-MS, so that different experimental approaches (e.g.,
530 direct sampling of the fluid in a reaction cell autoclave such as the design of Seyfried et al.
531 (1979)) need to be applied.
532

533 **Acknowledgments**

534 We thank Dionysis Foustoukos for editorial handling as well as two anonymous reviewers,
535 whose critical reviews of an earlier version significantly improved this manuscript. We
536 thank U. Kropp for his technical support as well as J. Feige for sample preparation. We are
537 grateful for helpful discussions with P. Lecumberri-Sanchez and R. Linnen. This work was
538 funded by the State of Lower Saxony (Germany), Graduate School GeoFluxes as well as the
539 Leibniz Universität Hannover.
540

Figures

Figure 1: Different capsule designs: a) with quartz cylinder, which was pre-fractured at 350°C and put into concentrated HF for 10 min, b) with quartz cylinder etched in concentrated HF for 30 min, c) with two quartz cylinders, one of which was pre-treated as in a) and the other was cleaned in HCl only; note that all capsules were crimped in the center, so that the quartz cylinder(s) were not in direct contact with the other phases of the experimental charge prior to the experiment. All capsules contained aqueous fluid with different NaCl concentrations, molybdenite and/or scheelite as Mo and W source respectively, silicagel to enhance quartz heeling as well as the mineral assemblage Pyrite-Pyrrhotite-Magnetite to buffer fO_2 and fS_2 (PPM buffer). Gold capsules served as a source for Au in the experiments.

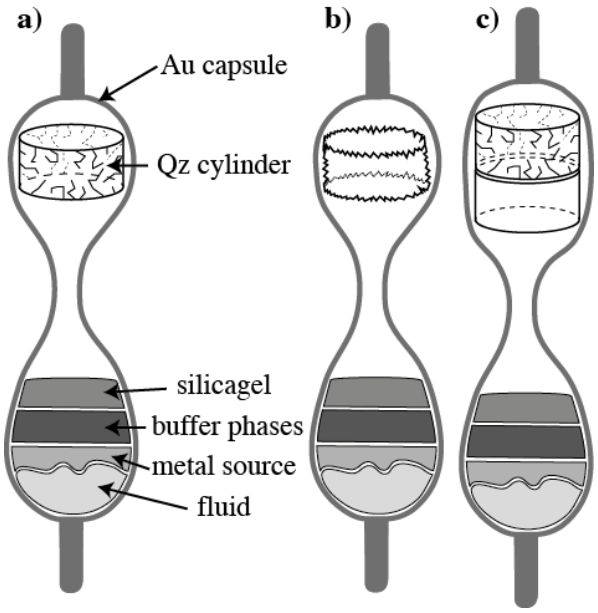

Figure 2: Typical LA-ICP-MS signal from a frozen fluid inclusion (metal source: molybdenite + scheelite + gold, formed at 800°C, 200 MPa, PPM buffer) using a UV-fs-laser, heating-freezing cell and *Element XR* ICP-MS.

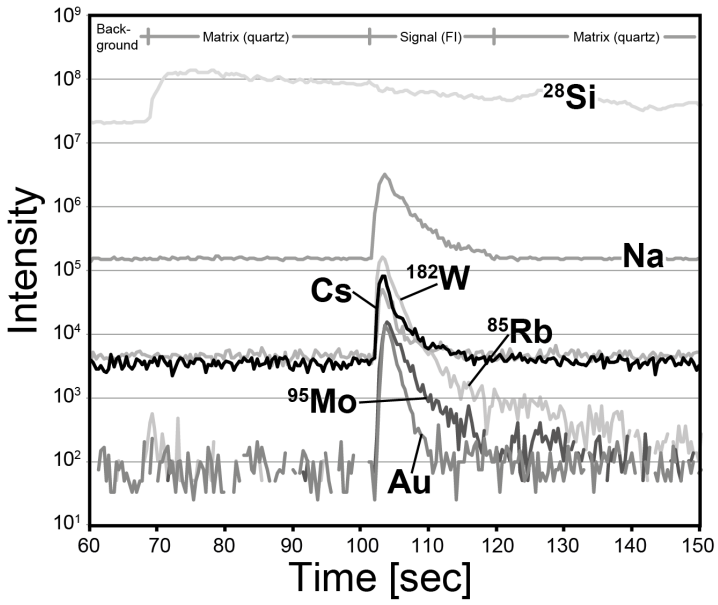

Figure 3: Typical appearance of synthetic fluid inclusions formed (a) at 600°C and 200 MPa in quartz that was only pre-cracked at 350°C, (b) at 600°C and 200 MPa in quartz that was pre-cracked at 350°C and immersed in concentrated HF for 10 minutes, (c, d) in-situ by an intermediate quench in a previously unfractured quartz at (c) 800°C and (d) 600°C and 200MPa.

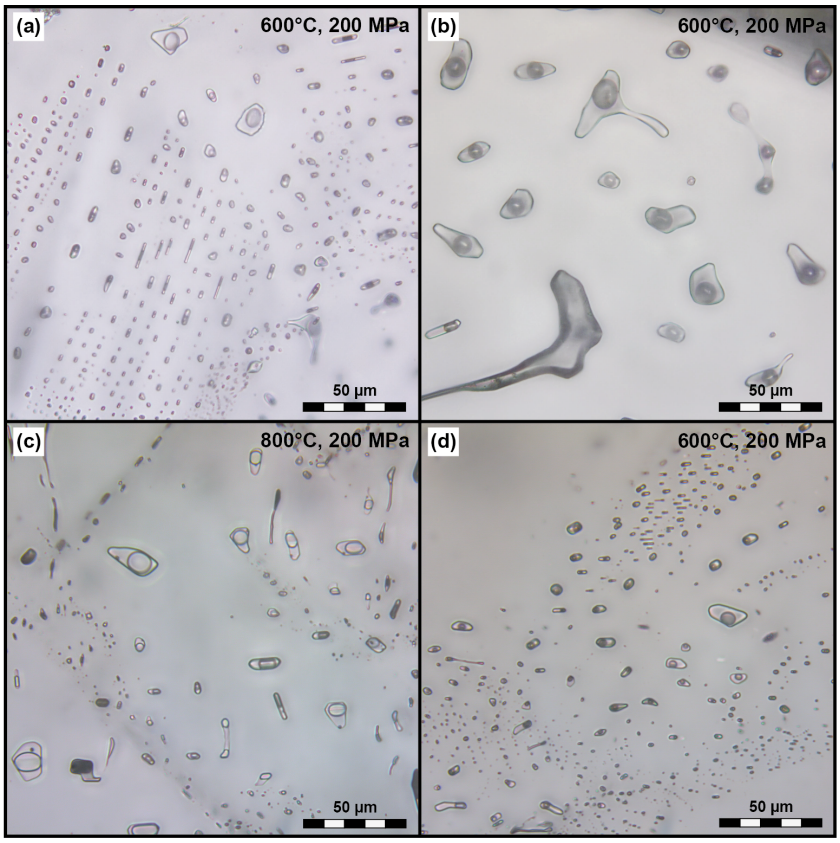

564 Figure 4: Polished section of quartz chip from pressure cycling *experiment A*. Note the convex
565 top and bottom faces of the cylinder, which were roughly parallel to each other prior to the
566 experiment.
567

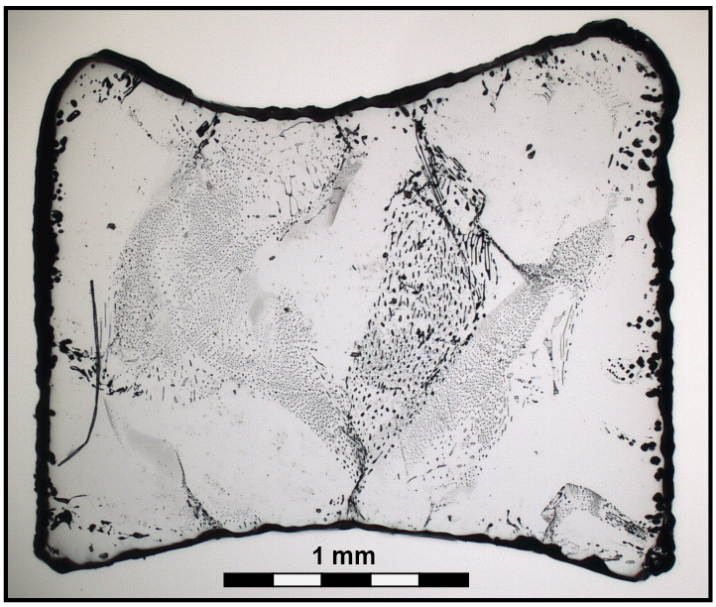

568

Figure 5: Results from setup 1 (equilibrations tests) using different approaches: Fluid concentrations of W from scheelite dissolution, Mo from molybdenite dissolution and Au from metallic gold dissolution at 800°C, 200 MPa and fO_2 and fS_2 conditions buffered by Pyrite-Pyrrhotite-Magnetite (PPM). ***Experiment A***: results from pressure cycling experiment (150 MPa to 250 MPa for five times every 10 minutes for 8 hours, followed by 3 days at 200 MPa) with pre-cracked (350°C to room temperature) and pre-etched (10 min in concentrated HF) quartz cylinder, ***Experiment B***: results from experiment with pre-etched (30 min in concentrated HF) quartz cylinder and intermediate quench (2 + 3 days), ***Experiment C***: results from experiment with two quartz cylinders (left/top: pre-cracked and pre-etched (350°C to room temperature followed by 10 min in concentrated HF), right/bottom: not pre-treated) and intermediate quench (2 + 3 days), **Literature Data**: *1) W concentration extrapolated to 800°C using data from Foster (1977, 252-529°C, 100-200 MPa, muscovite – K-feldspar – quartz buffer + 1 M KCl, metal source was also scheelite), *2) measured Mo concentration from Zhang et al. (2012, 800°C, 200 MPa, PPM buffer, 8 wt% NaCl, metal source: molybdenite), *3) Au concentration extrapolated to 800°C using data from Loucks and Mavrogenes (1999, 625-725°C, 110 MPa, PPM buffer, 1 m HCl, metal source: metallic gold).

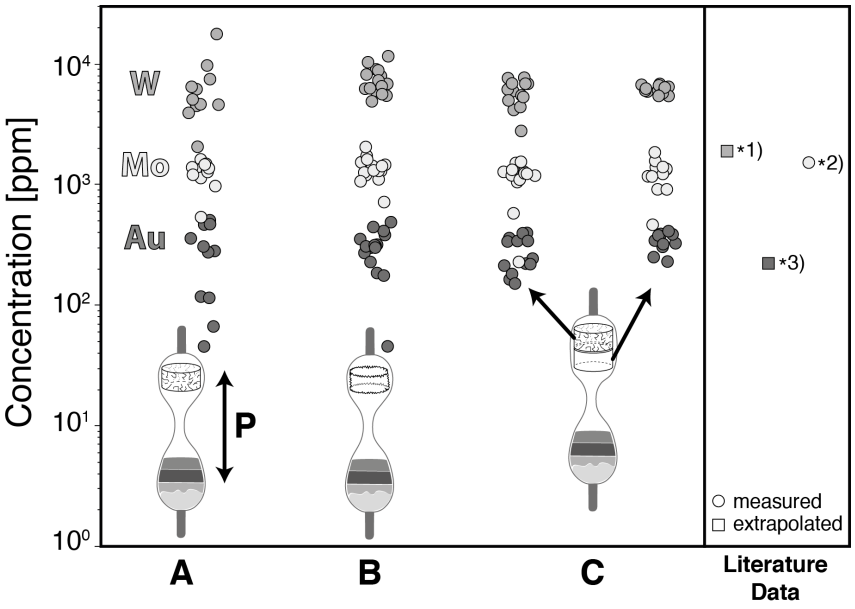
Concentration [ppm]
10^4
10^3
10^2
10^1
10^0
W
Mo
Au
P
A
B
C
Literature Data
*1)
*2)
*3)
measured
extrapolated

586

Figure 6: A) Strategy applied to test the role of intermediate quench on fluid inclusion formation (setup 2). From left to right: 1. Formation of fluid inclusions in pre-treated (pre-cracked at 350°C and immersed in concentrated HF for 10 minutes) quartz cylinder at 600°C (200 MPa) – 2. Intermediate quench of the sample from 600°C to room temperature, leading to the formation of new cracks and opening of some of the early formed fluid inclusions – 3. Formation of new and refilled fluid inclusions at 400°C by healing of the newly formed cracks. B) Results from setup 2: Measured homogenization temperatures (T_{hom}) of fluid inclusions in our three samples versus fluid salinity (white circles). Grey circles depict calculated T_{hom} for 400°C (light grey) and 600°C (dark grey) and 200 MPa for the different fluid salinities after Driesner and Heinrich (2007) and Driesner (2007).

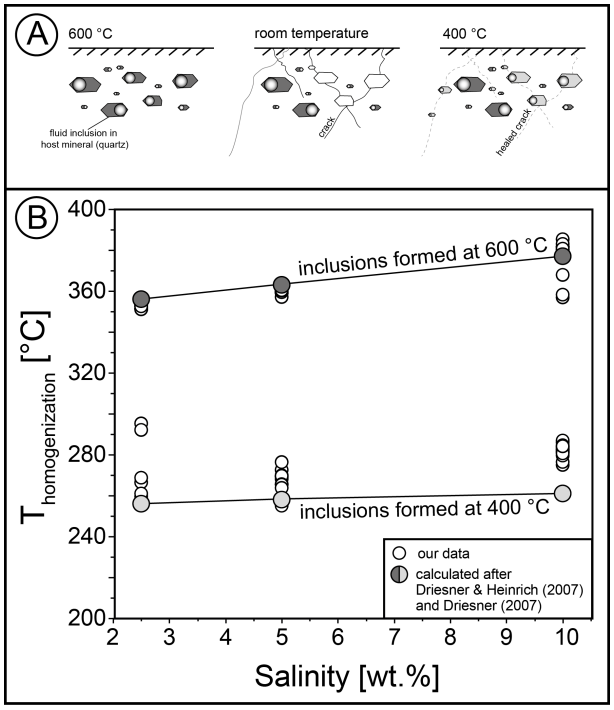

599 Figure 7: Results from setup 3 (time dependent experiments): concentrations of W from scheelite
600 dissolution (grey circles), Mo from molybdenite dissolution (light grey circles) and Au (dark grey
601 circles) from native gold dissolution after different runtimes (1.8 to 100 h) at 800°C, 200 MPa
602 and fO_2 and fS_2 conditions buffered by the PPM buffer. Transparent lines roughly trace the
603 development of maximum metal concentrations with time. See text for discussion of initially
604 higher Mo values (indicated by dashed line).
605

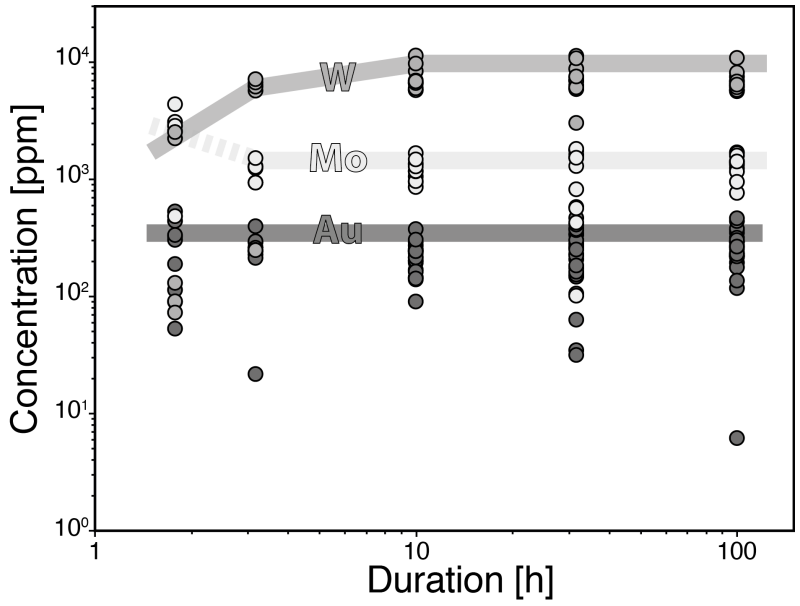

606

Tables

Table 1: Summary of experiments from setup 1 and respective results. W, Mo and Au concentrations are given in ppm by weight.

#	Type	T [°C]	P [MPa]	Composition	$logfO_2$ [bar]	$logfS_2$ [bar]	n	W [ppm] in fluid		Mo [ppm] in fluid		Au [ppm] in fluid	
								Avg	Stdev	Avg	Stdev	Avg	Stdev
A	P-cycling	800	200	8 wt% NaCl, Mol, Sch, PPM	-11.2	0.4	11	6370	4000	1320	180	270	160
B	HF pre-treatment	800	200	8 wt% NaCl, Mol, Sch, PPM	-11.2	0.4	16	7370	1740	1400	250	330	80
C_1	350°C + HF	800	200	8 wt% NaCl, Mol, Sch, PPM	-11.2	0.4	13	5900	1280	1260	140	280	90
C_2	not pre-treated	800	200	8 wt% NaCl, Mol, Sch, PPM	-11.2	0.4	12	6100	470	1290	270	330	60

n: number of analyzed fluid inclusions after discarding analysis with Cs/Rb and Na/Rb ratios deviating by more than 10 % and 20% of the initial fluid, respectively.

8 wt% NaCl, Mol, Sch, PPM: Fluid with 8 wt% NaCl coexisting with molybdenite, scheelite and PPM buffer

$logfO_2$, $logfS_2$: according to Zhang et al. (2012)

$logfO_2$ of -11.2 corresponds to NNO +2.5 at 800°C and 200 MPa

Table 2: Homogenization temperatures from pre-cracked and etched quartz cylinders from setup 2. Experiments were run as described in the text at 200 MPa with three different salinities at 600°C prior and 400°C after the intermediate quench. Calculated temperatures were obtained from the SoWat model of Driesner and Heinrich (2007) and Driesner (2007).

Sample	#	Salinity [wt% NaCl]	T_{hom} [°C]	Sample	#	Salinity [wt% NaCl]	T_{hom} [°C]	Sample	#	Salinity [wt% NaCl]	T_{hom} [°C]
ID 145	1	2.5	266	ID 146	1	5	273	ID 147	1	10	281
	2	2.5	351		2	5	360		2	10	385
	3	2.5	351		3	5	359		3	10	382
	4	2.5	352		4	5	359		4	10	382
	5	2.5	354		5	5	360		5	10	275
	6	2.5	269		6	5	361		6	10	276
	7	2.5	352		7	5	360		7	10	382
	8	2.5	351		8	5	270		8	10	382
	9	2.5	352		9	5	276		9	10	282
	10	2.5	352		10	5	359		10	10	284
	11	2.5	352		11	5	268		11	10	n.d.
	12	2.5	351		12	5	359		12	10	n.d.
	13	2.5	351		13	5	269		13	10	283
	14	2.5	351		14	5	359		14	10	283
	15	2.5	354		15	5	359		15	10	284
	16	2.5	353		16	5	360		16	10	282
	17	2.5	353		17	5	255		17	10	357
	18	2.5	353		18	5	269		18	10	358
	19	2.5	353		19	5	n.d.		19	10	281
	20	2.5	353		20	5	357		20	10	280
	21	2.5	260		21	5	362		21	10	281
	22	2.5	261		22	5	361		22	10	286
	23	2.5	355		23	5	359		23	10	287
	24	2.5	353		24	5	270		24	10	285
	25	2.5	n.d.		25	5	360		25	10	284
	26	2.5	295		26	5	360		26	10	368
	27	2.5	353		27	5	360		27	10	380
	28	2.5	292		28	5	266		28	10	380
	29	2.5	n.d.		29	5	265		29	10	383
	30	2.5	353		30	5	264		30	10	381
calculated (400°C, 200MPa)		2.5	256	calculated (400°C, 200MPa)		5	258	calculated (400°C, 200MPa)		10	261
calculated (600°C, 200MPa)		2.5	356	calculated (600°C, 200MPa)		5	364	calculated (600°C, 200MPa)		10	378

622 Table 3: Results from the time dependent series from setup 3. All experiments were run at 800
623 °C, 200 MPa with an 8 wt% NaCl fluid and buffered by the PPM buffer. The sources for the
624 metals were native gold of the capsule material and molybdenite or scheelite, respectively.
625

	Molybdenite Series			Scheelite Series		
Duration [h]	**Sample**	**Mo [ppm]**	**Au [ppm]**	**Sample**	**W [ppm]**	**Au [ppm]**
100	ID 191	1370	272	ID 192	5610	229
		1686	365		6175	220
		1419	347		5723	234
		1355	254		6377	221
		1317	262		6905	289
		754	6		7468	290
		1158	294		6620	300
		1652	377		10792	117
		1582	437		5758	176
		1231	193		8097	218
		1406	461		6061	229
		1157	223		6793	265
		1408	293		6382	136
		760	215			
		945	315			
31.6	ID 194	1527	464	ID 193	6282	63
		1749	340		3007	280
		1515	300		8687	105
		1612	365		6968	333
		575	174		7374	bdl
		816	161		8710	146
		1288	221		5920	257
		562	182		11239	206
		1773	374		5847	153
		1805	408		6849	265
		101	bdl		6961	300
		424	31		6039	34
		1516	250		10707	229
					7492	380
10	ID 195	1660	240	ID 197	6537	270
		939	144		14755	90
		1336	290		8311	373
		bdl	bdl		5764	201
		1350	144		5726	162
		1049	168		6918	139
		853	250		5935	214
		958	201		6647	242
		1160	193		6587	251
		1166	243		6810	242
		1277	213		11308	141
		1468	233		9661	303

3.17	ID 196	1285	240	ID 198	6335	212
		1238	288		247	22
		931	239		5672	bdl
		1267	260		6135	293
		1506	395		6655	258
		930	226		7105	248
1.78	ID 200	4340	302	ID 199	2221	323
		2567	528		130	53
		3067	332		2512	438
		2840	188		90	113
		481	89		72	bdl

626 *bdl: below detection limit
627

References

Akinfiev, N.N., and Diamond, L.W. (2009) A simple predictive model of quartz solubility in water-salt-CO2 systems at temperatures up to 1000 degrees C and pressures up to 1000 MPa. Geochimica Et Cosmochimica Acta, 73(6), 1597-1608.

Albrecht, M., Derrey, I.T., Horn, I., Schuth, S., and Weyer, S. (2014) Quantification of trace element contents in frozen fluid inclusions by UV-fs-LA-ICP-MS analysis. Journal of Analytical Atomic Spectrometry, 29(6), 1034-1041.

Benning, L.G., and Seward, T.M. (1996) Hydrosulphide complexing of Au(I) in hydrothermal solutions from 150-400 degrees C and 500-1500bar. Geochimica Et Cosmochimica Acta, 60(11), 1849-1871.

Berndt, J., Holtz, F., and Koepke, J. (2001) Experimental constraints on storage conditions in the chemically zoned phonolitic magma chamber of the Laacher See volcano. Contributions to Mineralogy and Petrology, 140(4), 469-486.

Berry, A.J., Hack, A.C., Mavrogenes, J.A., Newville, M., and Sutton, S.R. (2006) A XANES study of Cu speciation in high-temperature brines using synthetic fluid inclusions. American Mineralogist, 91(11-12), 1773-1782.

Bodnar, R.J., Burnham, C.W., and Sterner, S.M. (1985) Synthetic Fluid Inclusions in Natural Quartz. III. Determination of Phase-Equilibrium Properties in the System H2O-NaCl to 1000 °C and 1500 bars. Geochimica et Cosmochimica Acta, 49(9), 1861-1873.

Driesner, T. (2007) The system H2O-NaCl. Part II: Correlations for molar volume, enthalpy, and isobaric heat capacity from 0 to 1000 degrees C, 1 to 5000 bar, and 0 to 1 X-NaCl. Geochimica Et Cosmochimica Acta, 71(20), 4902-4919.

Driesner, T., and Heinrich, C.A. (2007) The system H2O-NaCl. Part I: Correlation formulae for phase relations in temperature-pressure-composition space from 0 to 1000 degrees C, 0 to 5000 bar, and 0 to 1 X-NaCl. Geochimica Et Cosmochimica Acta, 71(20), 4880-4901.

Duc-Tin, Q., Audetat, A., and Keppler, H. (2007) Solubility of tin in (Cl, F)-bearing aqueous fluids at 700 degrees C, 140 MPa: A LA-ICP-MS study on synthetic fluid inclusions. Geochimica Et Cosmochimica Acta, 71(13), 3323-3335.

Eugster, H.P. (1957) Heterogeneous Reactions Involving Oxidation and Reduction at High Pressures and Temperatures. Journal of Chemical Physics, 26(6), 1760-1761.

Foster, R.P. (1977) Solubility of Scheelite in Hydrothermal Chloride Solutions. Chemical Geology, 20(1), 27-43.

Frank, M.R., Simon, A.C., Pettke, T., Candela, P.A., and Piccoli, P.M. (2011) Gold and copper partitioning in magmatic-hydrothermal systems at 800 degrees C and 100 MPa. Geochimica Et Cosmochimica Acta, 75(9), 2470-2482.

Gibert, F., Pascal, M.L., and Pichavant, M. (1998) Gold solubility and speciation in hydrothermal solutions: Experimental study of the stability of hydrosulphide complex of gold (AuHS degrees) at 350 to 450 degrees C and 500 bars. Geochimica Et Cosmochimica Acta, 62(17), 2931-2947.

Guillong, M., and Heinrich, C.A. (2007) Sensitivity enhancement in laser ablation ICP-MS using small amounts of hydrogen in the carrier gas. Journal of Analytical Atomic Spectrometry, 22(12), 1488-1494.

Guillong, M., Meier, D., Allan, M., Heinrich, C., and Yardley, B. (2008) SILLS: a MATLAB-based program for the reduction of laser ablation ICP-MS data of homogeneous materials and inclusions. Mineralogical Association of Canada Short Course, 40, 328-333.

674 Günther, D., Audetat, A., Frischknecht, R., and Heinrich, C.A. (1998) Quantitative analysis of
675 major, minor and trace elements in fluid inclusions using laser ablation inductively
676 coupled plasma mass spectrometry. Journal of Analytical Atomic Spectrometry,
677 13(4), 263-270.
678 Hack, A.C., and Mavrogenes, J.A. (2006) A synthetic fluid inclusion study of copper solubility
679 in hydrothermal brines from 525 to 725 degrees C and 0.3 to 1.7 GPa. Geochimica Et
680 Cosmochimica Acta, 70(15), 3970-3985.
681 Hanley, J.J., Pettke, T., Mungall, J.E., and Spooner, E.T.C. (2005) The solubility of platinum
682 and gold in NaCl brines at 1.5 kbar, 600 to 800 degrees C: A laser ablation ICP-MS
683 pilot study of synthetic fluid inclusions (vol 10, pg 2593, 2005). Geochimica Et
684 Cosmochimica Acta, 69(23), 5635-5637.
685 Heinrich, C., Günther, D., Audétat, A., Ulrich, T., and Frischknecht, R. (1999) Metal
686 fractionation between magmatic brine and vapor, determined by microanalysis of
687 fluid inclusions. Geology, 27(8), 755-758.
688 Jochum, K.P., Nohl, L., Herwig, K., Lammel, E., Toll, B., and Hofmann, A.W. (2005) GeoReM: A
689 new geochemical database for reference materials and isotopic standards.
690 Geostandards and Geoanalytical Research, 29(3), 333-338.
691 Lerchbaumer, L., and Audetat, A. (2009) Partitioning of Cu between vapor and brine - An
692 experimental study based on LA-ICP-MS analysis of synthetic fluid inclusions.
693 Geochimica Et Cosmochimica Acta, 73(13), A744-A744.
694 Li, Y., and Audetat, A. (2009) A method to synthesize large fluid inclusions in quartz at
695 controlled times and under unfavorable growth conditions. American Mineralogist,
696 94(2-3), 367-371.
697 Loucks, R.R., and Mavrogenes, J.A. (1999) Gold solubility in supercritical hydrothermal
698 brines measured in synthetic fluid inclusions. Science, 284(5423), 2159-2163.
699 Matthews, W., Linnen, R.L., and Guo, Q. (2003) A filler-rod technique for controlling redox
700 conditions in cold-seal pressure vessels. American Mineralogist, 88(4), 701-707.
701 Newton, R.C., and Manning, C.E. (2000) Quartz solubility in H2O-NaCl and H2O-CO2
702 solutions at deep crust-upper mantle pressures and temperatures: 2-15 kbar and
703 500-900 degrees C. Geochimica Et Cosmochimica Acta, 64(17), 2993-3005.
704 Pokrovski, G.S., Kokh, M.A., Guillaume, D., Borisova, A.Y., Gisquet, P., Hazemann, J.L., Lahera,
705 E., Del Net, W., Proux, O., Testemale, D., Haigis, V., Jonchiere, R., Seitsonen, A.P., Ferlat,
706 G., Vuilleumier, R., Saitta, A.M., Boiron, M.C., and Dubessy, J. (2015) Sulfur radical
707 species form gold deposits on Earth. Proceedings of the National Academy of
708 Sciences of the United States of America, 112(44), 13484-13489.
709 Roedder, E., and Kopp, O.C. (1975) A check on the validity of the pressure correction in
710 inclusion geothermometry, using hydrothermally grown quartz. Fortschr. Miner., 52,
711 431-446.
712 Seo, J.H., Guillong, M., Aerts, M., Zajacz, Z., and Heinrich, C.A. (2011) Microanalysis of S, Cl,
713 and Br in fluid inclusions by LA-ICP-MS. Chemical Geology, 284(1-2), 35-44.
714 Seyfried, W.E., Gordon, P.C., and Dickson, F.W. (1979) New Reaction Cell for Hydrothermal
715 Solution Equipment. American Mineralogist, 64(5-6), 646-649.
716 Shelton, K.L., and Orville, P.M. (1980) Formation of Synthetic Fluid Inclusions in Natural
717 Quartz. American Mineralogist, 65(11-1), 1233-1236.
718 Simon, A.C., Frank, M.R., Pettke, T., Candela, P.A., Piccoli, P.M., Heinrich, C.A., and Glascock,
719 M. (2007) An evaluation of synthetic fluid inclusions for the purpose of trapping

equilibrated, coexisting, immiscible fluid phases at magmatic conditions. American Mineralogist, 92(1), 124-138.
Simon, A.C., Pettke, T., Candela, P.A., Piccolli, P.M., and Heinrich, C.A. (2006) Copper partitioning in a melt-vapor-brine-magnetite-pyrrhotite assemblage. Geochimica Et Cosmochimica Acta, 70(22), 5583-5600.
Sterner, S.M., and Bodnar, R.J. (1984) Synthetic Fluid Inclusions in Natural Quartz .1. Compositional Types Synthesized and Applications to Experimental Geochemistry. Geochimica Et Cosmochimica Acta, 48(12), 2659-2668.
Sterner, S.M., Hall, D.L., and Bodnar, R.J. (1988) Synthetic Fluid Inclusions. V. Solubility Relations in the System NaCl-KCl-H2O under Vapor-Saturated Conditions. Geochimica Et Cosmochimica Acta, 52(5), 989-1005.
Ulrich, T., and Mavrogenes, J. (2008) An experimental study of the solubility of molybdenum in H2O and KCl-H(2)Osolutions from 500 degrees C to 800 degrees C, and 150 to 300 MPa. Geochimica Et Cosmochimica Acta, 72(9), 2316-2330.
Zajacz, Z., Seo, J.H., Candela, P.A., Piccoli, P.M., Heinrich, C.A., and Guillong, M. (2010) Alkali metals control the release of gold from volatile-rich magmas. Earth and Planetary Science Letters, 297(1-2), 50-56.
Zhang, L., Audetat, A., and Dolejs, D. (2012) Solubility of molybdenite (MoS2) in aqueous fluids at 600-800 degrees C, 200 MPa: A synthetic fluid inclusion study. Geochimica Et Cosmochimica Acta, 77, 175-185.